Stability of boron- and gallium-induced surface structures on Si(111) during deposition and epitaxial growth of silicon

R. L. Headrick, L. C. Feldman, and I. K. Robinson
AT&T Bell Laboratories, Murray Hill, New Jersey 07974

(Received 13 March 1989; accepted for publication 29 May 1989)

We have undertaken a new set of experiments to investigate the behavior of adsorbed-impurity induced reconstructions at growth interfaces. We have observed a striking difference in the stability of the B$\sqrt{3}\times\sqrt{3}$ and Ga$\sqrt{3}\times\sqrt{3}$ two-dimensional structures at the interface between Si(111) and *a*-Si, and in their segregation behavior during molecular beam epitaxy crystal growth. This leads to a new model of dopant behavior in silicon molecular beam epitaxy.

The atomic geometry of ordered adsorbate structures at crystal surfaces is well established for many cases; however, the effect of subsequent crystal growth on the adsorbate distribution is not well understood. Dopant redistribution is an important limitation in the design of new materials structures by modern epitaxial growth techniques. For example, confinement along the growth direction is the basis of "δ doping" of GaAs (by Si or Be) in molecular beam epitaxy (MBE) where impurities are retained within a few monolayers of an interface.[1] In some favorable cases, it may be possible to preserve an ordered array of adsorbates during the growth of an epitaxial overlayer[2]; this requires that there is no redistribution either in the growth direction or "in-plane." The possibility of preserving an ordered adsorbate structure at a buried epitaxial interface raises exciting possibilities for new materials.

In this letter, we explore the in-plane redistribution and surface segregation of the two column III elements, boron and gallium, on Si(111) using x-ray diffraction (XRD), Auger electron spectroscopy (AES), low-energy electron diffraction (LEED), and Rutherford backscattering spectroscopy (RBS). The results show that the gallium $\sqrt{3}\times\sqrt{3}$ structure is unstable with respect to the addition of Si adatoms. Boron is stable on Si(111) with respect to room-temperature deposition of Si adatoms, and is incorporated into crystalline silicon up to a limited concentration for high-temperature silicon deposition. The results are explained in terms of the different atomic sites occupied by boron and gallium in their respective $\sqrt{3}\times\sqrt{3}$ structures.

Samples were prepared in a MBE chamber equipped with an electron gun evaporator to deposit silicon, a quartz-crystal thickness monitor, and a Knudsen cell to deposit either gallium from elemental Ga or boron from HBO_2. LEED and Auger analysis were performed *in situ* and x-ray diffraction analysis was done after removing samples from the MBE chamber. The x-ray diffraction equipment was a four-circle diffractometer with a rotating anode source and a graphite monochromator. The Ga $\sqrt{3}\times\sqrt{3}$ surface reconstruction was prepared by deposition of 1/3 monolayer (ML) of Ga while the sample was held at 550 °C. The boron $\sqrt{3}\times\sqrt{3}$ surface reconstruction was prepared either by surface segregation of 1/3 ML of boron[3] from boron-implanted samples at 900 °C, or by deposition of boron onto *n*-type samples from HBO_2 while the sample was held at 750 °C.[4] The samples that were prepared by boron deposition were used to measure the boron coverages in the B $\sqrt{3}\times\sqrt{3}$ structure by the $B^{11}(p,\alpha)Be^8$ nuclear reaction method.[5]

Figure 1 shows LEED patterns for the Ga $\sqrt{3}\times\sqrt{3}$ surface structure and the B $\sqrt{3}\times\sqrt{3}$ surface structure. After ≈ 1 Å of Si deposition on these surfaces at room temperature, LEED patterns (c) and (d) were observed. The Ga superstructure disappears, while the B $\sqrt{3}\times\sqrt{3}$ is still clearly visible. Further LEED experiments showed that the Ga $\sqrt{3}\times\sqrt{3}$ disappeared between 0.3 and 0.4 ML silicon coverage (approximately one silicon atom for each gallium atom). Gallium is not desorbed from the surface by silicon deposition (this was confirmed by RBS and AES measurements), so it must be randomly arranged rather than in a periodic structure. In contrast, boron remains in a well-ordered $\sqrt{3}\times\sqrt{3}$ structure even in the presence of excess surface silicon.

This conclusion has been verified by deposition of 50 Å of *a*-Si on Si(111)Ga $\sqrt{3}\times\sqrt{3}$ and Si(111)B $\sqrt{3}\times\sqrt{3}$ surfaces and subsequent *ex situ* x-ray diffraction analysis. The two-dimensional nature of the buried boron $\sqrt{3}\times\sqrt{3}$ structure results in a diffraction "rod" that is independent of *l*, the mo-

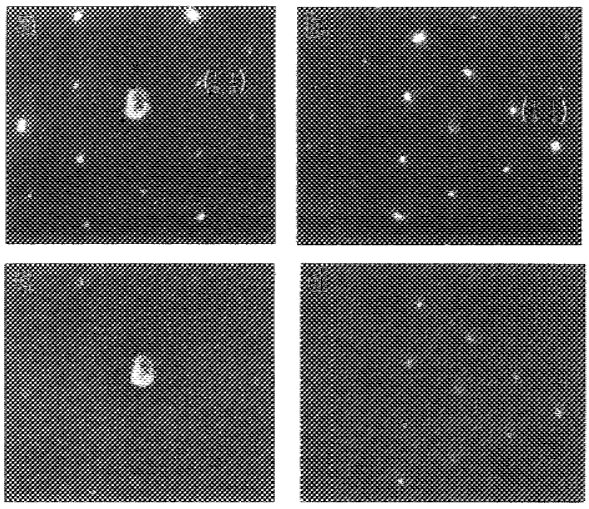

FIG. 1. LEED patterns for (a) Ga$\sqrt{3}\times\sqrt{3}$ on Si(111) at 66 eV, (b) B$\sqrt{3}\times\sqrt{3}$ on Si(111) at 82 eV, (c) and (d) same as (a) and (b), respectively, but with 1 Å of *a*-Si deposited at room temperature.

 0003-6951/89/310442-03$01.00

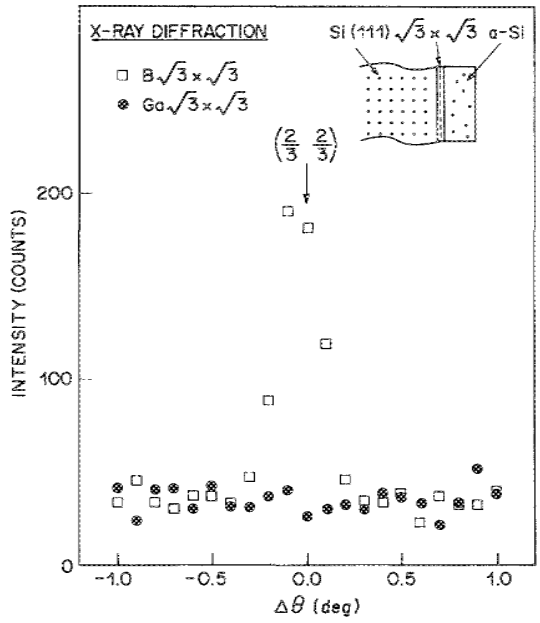

FIG. 2. Rocking scan through the (2/3,2/3) surface x-ray diffraction rod for buried boron and gallium surface structures on Si(111).

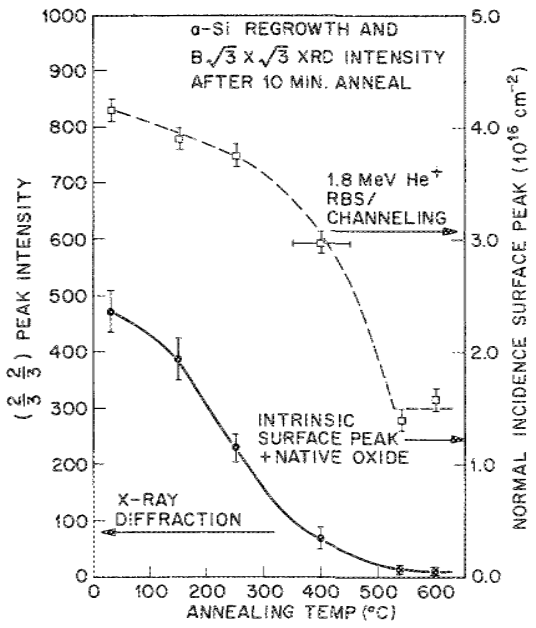

FIG. 3. Temperature dependence of the (2/3,2/3) surface x-ray diffraction integrated intensity as a function of annealing temperature for buried boron $\sqrt{3}\times\sqrt{3}$ surface structures (filled in circles). Temperature dependence of normal incidence channeling surface peak intensities for the buried boron $\sqrt{3}\times\sqrt{3}$ structure (open squares).

mentum transfer perpendicular to the surface. Figure 2 shows rocking scans through the (2/3,2/3) diffraction rod at $l = 0.2$. The rod is indexed relative to the surface unit cell as LEED patterns are indexed; to this end we define a hexagonal unit cell for Si.[6] A clear signal is obtained from the Si(111)B $\sqrt{3}\times\sqrt{3}$/a-Si structure, but not from the corresponding gallium structure.

Annealing of B $\sqrt{3}\times\sqrt{3}$ samples capped with 58 Å of amorphous silicon results in a decrease of the diffraction intensity from the two-dimensional interface structure and epitaxial growth (crystallization) of the amorphous silicon. Figure 3 shows the (2/3,2/3) diffraction intensity and the normal incidence Si RBS surface peak for five different samples as a function of annealing temperature. A large decrease in the Si surface peak intensity is observed for annealing temperatures $\geqslant$400 °C, illustrating the crystallization. Samples annealed at 540 and 600 °C exhibited 7×7 LEED patterns before they were removed from the MBE chamber. For these samples, a small but finite amount (2–3%) of the original 1/3 order diffraction signal remains. If boron is evenly distributed in the two-dimensional interface layer (on the scale of the x-ray coherence length), then the integrated intensity measured by the diffraction experiment is proportional to the square of the number of boron atoms on ordered sites. This suggests that as much as 14–17% ($\simeq 4\times10^{13}$ cm^{-2}) of the boron remains in an ordered $\sqrt{3}\times\sqrt{3}$ array. This ordered adsorbate structure also remains at the buried interface, since it is stable with respect to exposure to air for periods of several months with no noticeable degradation of the interface diffraction signal. It was recently reported that a small fraction of the reconstruction also remains at the interface during conventional molecular beam epitaxy growth of Si on the Si(111)B$\sqrt{3}\times\sqrt{3}$ structure grown at 600 °C.[2]

Auger measurements on varying thicknesses of a-Si overlayers on B $\sqrt{3}\times\sqrt{3}$ samples show that when Si is deposited at room temperature, surface boron is buried with no boron segregation or islanding of the deposited Si. Upon annealing at 540 °C, significant boron surface segregation is observed for overlayer thicknesses <50 Å. Thus, the decrease of the 1/3rd order diffraction signal can be attributed to redistribution of boron during annealing.

Further insight into the interaction between boron and silicon or gallium and silicon can be obtained from high-temperature Si deposition experiments. Figure 4 shows the surface concentrations of Ga and B (starting from 1/3 ML coverage) as a function of Si overlayer thickness. At the growth temperature of 540 °C, desorption of boron or gallium from Si(111) is negligible. Quite different segregation behavior is observed for the two species: boron exhibits a linearly decreasing concentration while Ga exhibits a constantly changing rate of decrease.

We propose the following model to explain the results of Fig. 4. For a given Si growth rate dx/dt, an amount dn_s/dt of surface impurity is incorporated according to $dn_s/dt = Kn_s^p dx/dt$. Integration gives

$$n_s(x) = n_s(0) - K_0 x \quad p = 0, \tag{1a}$$

$$n_s(x) = n_s(0)\exp(-K_1 x) \quad p = 1. \tag{1b}$$

Here $n_s(x)$ is the impurity concentration seen at the surface after Si growth to a thickness x. The constant K_0 is simply the effective solubility while K_1 is a first-order rate constant which is related to the trapping probability per site of an impurity atom (and is likely to depend on the growth rate). We have introduced the exponent p to represent the kinetic

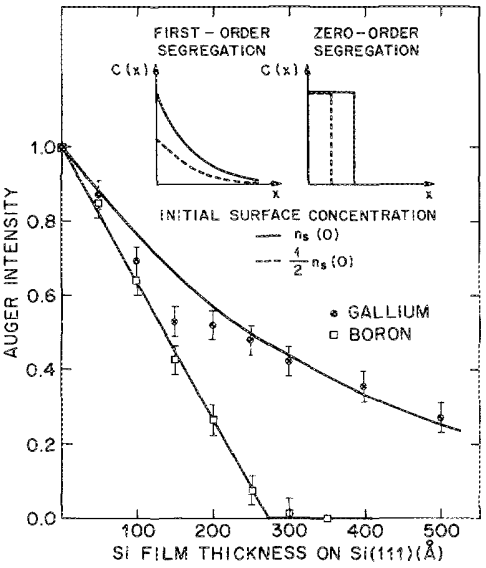

FIG. 4. Boron or gallium surface Auger intensity during conventional molecular beam epitaxy growth of Si on the impurity stabilized $\sqrt{3}\times\sqrt{3}$ surface structures. The growth rate was ≈ 0.1 Å/s. The insets show the impurity profiles resulting from zero- and first-order segregation during MBE growth.

order of segregation so that boron on Si(111) exhibits zero-order segregation, while gallium on Si(111) exhibits first-order segregation. Based on the observations illustrated by Figs. 1 and 2, we propose that gallium can be displaced from surface sites by mobile Si adatoms which are always present on the surface during molecular beam epitaxy crystal growth. The reactions on the surface responsible for impurity segregation and incorporation are then

$$\mathrm{Ga_{surf}} + \mathrm{Si_{ad}} \rightarrow \mathrm{Ga_{ad}} + \mathrm{Si_{surf}}, \tag{2a}$$

$$\mathrm{Ga_{ad}} \rightarrow \mathrm{Ga_{surf}}. \tag{2b}$$

These reactions lead directly to the observed first-order segregation of gallium on Si(111) during MBE crystal growth, i.e., the incorporated fraction is proportional to the surface concentration. Boron incorporation, on the other hand, cannot be described by a kinetically limited surface reaction since dn_s/dt is independent of surface boron concentration, but can be described by an effective solubility limit K_0.

This behavior is explained by the different sites occupied by boron and gallium in the B $\sqrt{3}\times\sqrt{3}$ and Ga $\sqrt{3}\times\sqrt{3}$ structures. It has recently been established by synchrotron x-ray diffraction that the boron occupies a subsurface (second layer) substitutional site.[7] The other column III elements Al, Ga, and In, however, occupy the T_4 adatom site above the surface.[8] It is intuitively clear that the subsurface substitutional site (boron) will not directly interact with deposited Si while the T_4 adatom site (gallium) will be readily displaced by deposited Si. The subsurface substitutional site of boron also immediately converts into a normal bulk substitutional site upon growth of a silicon overlayer[7]; this explains the observation that epitaxial silicon can be grown on top of the B $\sqrt{3}\times\sqrt{3}$ structure without disordering it completely.

Now consider the depth profile of impurities resulting from impurity segregation. The shape of the depth profile for zero- and first-order segregation is given by $C(x) = dn_s/dx$ and is illustrated in Fig. 4. The most interesting feature of these curves is that the model predicts for zero-order segregation that for $x > n_s(0)/K_0$, the concentration $C(x) = 0$. Thus, the profile becomes narrower for lower initial surface concentrations $n_s(0)$ and monolayer doping is predicted for $n_s(0) < K_0 d$, where d is the layer spacing. The value of K_0 from the slope of the boron data in Fig. 4 is $K_0 = 9\times10^{19}$ cm^{-3}, and the layer spacing is 3.14 Å. This implies that sharp (single monolayer) boron profiles are possible at a boron "δ doping" concentration of 2.7×10^{12} cm^{-2}.

The authors are indebted to R. T. Tung, J. M. Gibson, B. A. Davidson, E. F. Schubert, B. Spear, and S. Yalisove for valuable contributions.

[1] E. F. Schubert, Y. Horikoshi, and K. Ploog, Phys. Rev. B **32**, 1085 (1985).
[2] K. Akimoto, J. Mizuki, I. Hirosawa, T. Tatsumi, H. Hirayama, N. Aizaki, and J. Matsui, *Extended Abstracts of the 19th Conference on Solid State Devices and Materials* (Business Center for Academic Societies, Tokyo, 1987), p. 463.
[3] V. V. Korobtsov, V. G. Lifshits, and A. V. Zotov, Surf. Sci. **195**, 467 (1988).
[4] H. Hirayama, T. Tatsumi, and N. Aizaki, Surf. Sci. **193**, L47 (1988).
[5] L. C. Feldman and S. T. Picraux, in *Ion Beam Handbook for Materials Analysis*, edited by J. W. Mayer and E. Rimini (Academic, New York, 1977), p. 112.
[6] I. K. Robinson, W. K. Waskiewicz, R. T. Tung, and J. Bohr, Phys. Rev. Lett. **57**, 2714 (1986).
[7] R. L. Headrick, I. K. Robinson, E. Vlieg, and L. C. Feldman (unpublished).
[8] J. M. Nicholls, B. Reihl, and J. E. Northrup, Phys. Rev. B **35**, 4137 (1987).